

Research Article

Calculation of the Initial $^{53}\text{Mn}/^{55}\text{Mn}$ in Calcium-Aluminum Rich Inclusions in the Solar Wind Implantation Model

Glynn Bricker* 

Department of Chemistry & Physics, Purdue University Northwest, Westville, Indiana, USA

Abstract

Studies indicate that short-lived radionuclides (SLRs), including ^{53}Mn , were incorporated into Calcium-Aluminum Rich inclusions (CAIs) in ancient undisturbed primitive meteorites at the time the solar system was forming. In this study, the potential incorporation of ^{53}Mn into CAIs in accordance with the Solar Wind Implantation Model (SWIM) is investigated. In the SWIM model, radiogenic nuclei are made through solar energetic particle (SEP) nuclear reactions with target material in the proto-stellar atmospheres of proto-stars are whilst the proto-stars are in the accretion phase. The newly produced daughter nuclei are subsequently trapped in the magnetic field lines associated with the proto-stars. The radiogenic nuclei are then funneled into the X-region, and some fraction of these nascent nuclei are implanted into refractory matter which accretes towards the proto-star. Production rates daughter nuclei scale with ancient X-ray luminosities, which have been measured to be 100,000 times contemporary levels in T Tauri stars, yielding daughter nuclei produced at $\sim 10^5$ over contemporary levels. From the ancient enhanced SEP fluxes and refractory mass inflow rate found in the SWIM, we found the initial $^{53}\text{Mn}/^{55}\text{Mn}$ isotopic ratio ranged from 4×10^{-5} to 6×10^{-4} , when taking into account spectral flare variability.

Keywords

Radio-Nuclide, ^{53}Mn , Early Solar System, Solar Wind, CAI, Solar Wind Implantation Model, x-Wind, SWIM

1. Introduction

Primordial solar system materials, particularly high-temperature condensates such as calcium-aluminum rich inclusions (CAIs), contain the decay products of short-lived radionuclides (SLRs) with half-lives shorter than 5 million years. These include isotopes like ^{10}Be , ^{26}Al , ^{41}Ca , ^{53}Mn , and ^{60}Fe . While the presence of these radionuclides in early solar system materials is well-established, there is ongoing debate about the mechanism through which they were incorporated into the materials that eventually accreted to form meteorites (cf. Gounelle et al. [1]). Models for their production and subsequent incorporation into early solar system materials

invoke either a local formation scenario using the early Sun with a dramatically enhanced energetic particle activity or an extra-solar system origin. Desch et al. [2] proposed that ^{10}Be originated in an extra-solar nebula, suggesting that it was trapped in the core of a molecular cloud after being produced by galactic cosmic rays. In contrast, Lee et al. [3], Shu et al. [4], and Gounelle et al. [5] support an X-wind irradiation model, where isotopes such as ^7Be , ^{10}Be , ^{26}Al , ^{36}Cl , ^{41}Ca , and ^{53}Mn are generated in situ. In this scenario, refractory rock material in the X-region of the protoplanetary disk is irradiated by solar energetic particles (see also Shu et al. [6]).

*Corresponding author: gbricker@pnw.edu (Glynn Bricker)

Received: 17 October 2024; **Accepted:** 12 November 2024; **Published:** 29 November 2024



Copyright: © The Author(s), 2024. Published by Science Publishing Group. This is an **Open Access** article, distributed under the terms of the Creative Commons Attribution 4.0 License (<http://creativecommons.org/licenses/by/4.0/>), which permits unrestricted use, distribution and reproduction in any medium, provided the original work is properly cited.

Clues to the origin of SLRs can be discerned from the half-lives and possible production mechanisms. With a 53-day half-life [7], ^7Be likely formed locally. However, additional evidence is required to confirm its status among the short-lived radionuclides (SLRs) found in CAIs, as it has been detected in only a single CAI sample [8]. Since ^{10}Be is not generated by stellar nucleosynthesis [9], the source of ^{10}Be must be energetic particle interaction. Gounelle et al. [1, 5] and McKeegan et al. [10] suggest that ^{10}Be could not have originated from an extra-solar nebula, such as ^{10}Be in galactic cosmic rays (GCRs) or from the irradiation of the molecular cloud by GCRs. They propose that the most likely source of ^{10}Be is from solar energetic particle irradiation. For the most massive of the SLRs, ^{60}Fe , the reaction $^{64}\text{Ni} (p, p\alpha)^{60}\text{Fe}$ produces ^{60}Fe , but the cross-section (< 0.1 mbarn for energies $< 200\text{MeV}$) is small and the target concentration is depleted in refractory materials leaving a predicted $^{60}\text{Fe}/^{56}\text{Fe}$ of the order $\sim 10^{-11}$ [11, 3], much lower than the measured ratio of $\sim 10^{-6}$. It is generally accepted that ^{60}Fe has an extra-solar system origin (c.f. Mostefaoui et al. [12]). The sources of the other radionuclides could differ and may include stellar processes. These processes could include asymptotic giant branch or Wolf-Rayet stars, or supernovae. Alternatively, they could result from interactions with energetic particles or a combination of these mechanisms.

In addition to the previously mentioned mechanisms for SLR incorporation, Bricker & Caffee [13-15] proposed the solar wind implantation model (SWIM) to account for the inclusion of ^7Be , ^{10}Be and ^{36}Cl in CAIs. Currently, ^{10}Be is produced in the Sun's atmosphere through spallation reactions, where energetic protons collide primarily with oxygen. This spallogenic ^{10}Be is then carried by the solar wind and implanted into solar system materials exposed to it. Nishiizumi and Caffee [16] detected solar-wind-implanted ^{10}Be in samples from an Apollo 17 trench, calculating the escape rate of ^{10}Be from the Sun's surface as approximately $0.13 \pm 0.05 \text{ }^{10}\text{Be cm}^{-2} \text{ s}^{-1}$. This result is consistent with theoretical estimates, which suggest that the time-averaged solar flare production rate of ^{10}Be at the Sun's surface is about $0.1 \text{ }^{10}\text{Be cm}^{-2} \text{ s}^{-1}$ [1].

The early solar system likely experienced higher production rates of ^{10}Be and other radionuclides. Feigelson et al. [17] and Wolk et al. [18] report X-ray luminosities of approximately $5 \times 10^{30} \text{ ergs s}^{-1}$ in T-Tauri stars. Such high X-ray luminosities correspond to particle fluxes vastly exceeding those observed in the modern Sun. The enhanced energetic particle flux, in turn, would lead to greater solar flare production of ^{10}Be . Bricker and Caffee [13-15] hypothesize that a portion of this outward-flowing ^{10}Be is incorporated into inward-flowing material, some of which eventually forms precursor materials for accretion. Using conservative estimates for the inward flow of material, the fraction of material dropping out of this funnel flow, and ^{10}Be production rates, Bricker & Caffee [13-15] can account for ^{10}Be and ^{36}Cl concentrations found in CAIs.

Studies reveal the one-time presence of ^{53}Mn in CAIs

(c.f.) (Shukolyukov and Lugmair [19]; Anand et al. [20]). Unlike the initial $^{26}\text{Al}/^{27}\text{Al}$ found in CAIs, which has a generally accepted canonical value (5×10^{-5}), the initial $^{53}\text{Mn}/^{55}\text{Mn}$ ratio is not well constrained and it is difficult to report a so called canonical value. Through statistical analysis of several samples, Desch et al [21] report an average value of 8×10^{-6} , and MacPherson et al [22] find the value to be $\sim 5 \times 10^{-5}$. In order to set a point of reference, we adopt 4×10^{-5} after Gounelle et al [5]. In this study, we examine the potential incorporation of ^{53}Mn into CAIs within primitive carbonaceous meteorites through the solar wind implantation model (SWIM). Table 1 below summarizes the characteristics of ^{53}Mn found in CAIs.

Table 1. Manganese Isotope Found in CAIs.

Nuclide	Half-life	Initial Reference Isotopic Ratio	Radionuclide (g^{-1})
^{53}Mn	3.7Myr	4×10^{-5}	4.6×10^{13}

2. Solar Wind Implantation Model

2.1. Overview

We investigate whether ^{53}Mn could have been generated in the solar nebula approximately 4.6 billion years ago via SEP bombardment of target materials in the proto-solar atmosphere. These short-lived radionuclides subsequently escape the solar atmosphere, carried by the solar wind. A portion of this outward-flowing SLRs, described as the effective outflow rate, becomes incorporated into the inward-flowing material from the protoplanetary accretion disk, described as the refractory mass inflow rate.

2.2. Ancient SLR Production Rates

We will use the SWIM developed by Bricker & Caffee [13-15] to calculate the concentration of ^{53}Mn in CAIs. The main target elements considered for these calculations are given in table 2 [23].

Table 2. Target elements used in modeling of production of short-lived radionuclides.

Isotope	Target Element	Projectile
^{53}Mn	Cr, Fe, Mn	p, α

Cosmogenic nuclides rates of production are calculated from the following formula:

$$p = \sum_i N_i \sum_j \int \sigma_{ij} \frac{dF(E)}{dE_j} dE \quad (1)$$

where i corresponds to the target element for the production of the specified daughter product, N_i represents the abundance of the target element (in units of g g^{-1}), j represents incident particles that sets in motion the nuclear reaction, $\sigma_{ij}(E)$ represents the cross section for the nuclear reaction which produces the daughter nuclide from incident particle j with energy E interacting with particle i for the given reaction (in cm^2). Here the differential energetic particle flux of particle j , corresponding to energy E , is $\frac{dF(E)}{dE_j}$ ($\text{cm}^{-2} \text{s}^{-1} \text{MeV}^{-1}$) [23].

The target material is taken to be in gaseous form, and with the same makeup as the Sun [24]. We assume the solar photosphere density to be about $1 \times 10^{-7} \text{g cm}^{-3}$ [25].

Reedy [24] found that for the present-day Sun, the energetic proton flux ($E > 10 \text{MeV}$) at 1 AU from the center of the Sun is approximately $200 \text{ protons cm}^{-2} \text{s}^{-1}$. This amount of activity is equivalent to $9.3 \times 10^6 \text{ protons cm}^{-2} \text{s}^{-1}$ at the face of the Sun. In reference to young Sun-type stars in early stages of formation, measurements of X-ray emissions from young stellar objects in the Orion Nebula Cluster (ONC) [17, 18] indicates average luminosities ranging from approximately $10^{30} \text{ ergs s}^{-1}$ to $10^{31} \text{ ergs s}^{-1}$. Assuming an average luminosity of $\sim 10^{30.3} \text{ ergs s}^{-1}$, Feigelson et al. [17] finds this value of luminosity corresponds to approximately a factor of 10^5 increase in SEP fluxes when comparing $\sim 1 \text{ Myr}$ pre-main sequence (PMS) stars like the Sun over main sequence stars similar to the Sun. Following Gounelle et al. [5], an X-ray luminosity of $5 \times 10^{30} \text{ ergs s}^{-1}$ corresponds to an energetic proton flux, with energies $E \geq 10 \text{ MeV}$, of approximately $1.9 \times 10^{10} \text{ cm}^{-2} \text{s}^{-1}$ at the X-region, a distance of 0.06 AU from the center of the Sun. In comparison to modern solar activity, this amount of energetic protons translates to a time averaged factor of 3.4×10^4 increase. Based on the Chandra X-ray luminosity measurements of ONC objects, this increase in particle fluxes—and consequently production rates—is plausible and may even be an underestimate. For SWIM calculations, we use an energetic particle flux of $3.7 \times 10^{12} \text{ protons cm}^{-2} \text{s}^{-1}$, for $E \geq 10 \text{MeV}$, at the solar surface. This is a factor of 4×10^5 increase in energetic protons when comparing ancient PMS Sun-like stars to the contemporary. Secondary neutrons produced from the incident nuclear reactions are stopped within a column density of 50 g cm^{-2} [3]. Taking into account the density of the photosphere and that the magnetic field will not confine neutrons, it is likely that the secondary neutrons will escape before interacting. We therefore ignore production from secondary neutrons. A discuss of the dependence of energetic particle fluxes and X-ray luminosity for PM Sun-like stars can be found in Bricker & Caffee [13].

We determine the rate of daughter nuclide production with the assumption that energetic protons adhere to a power law distribution:

$$\frac{dF}{dE} = kE^{-r} \quad (2)$$

The value of r is in the range from 2.5 to 4, and all power law exponents, $\alpha/H = 0.1$. In the case of impulsive flares, where $r = 4$, we assign ${}^3\text{He}/\text{H} = 0.1$ and ${}^3\text{He}/\text{H} = 0.3$. For flatter flares, where $r = 2.5$, we assign ${}^3\text{He}/\text{H} = 0$. It is understood that both the energetic particle flux and spectral exponents experience short- and long-term variations, making a detailed reconstruction of solar energetic particle fluxes and spectra impossible [26]. For the calculation of ${}^{53}\text{Mn}$ rates of production, we use the nuclear cross sections taken from To Gensho et al. [27], Ramaty et al. [28], and Leya et al. [11]. Whenever possible, experimental cross sections have been included with the goal of limiting any uncertainties associated which may arise from theoretically calculated nuclear cross sections. We approximate the uncertainty in the cross sections to be about a factor of two [11]. The reactions examined here represent the primary nuclear production pathways, factoring in both the availability of target matter and the robustness of nuclear cross sections. Any reactions not included in the potential nuclear reaction pathways are unlikely to significantly affect the overall rate of ${}^{53}\text{Mn}$ production.

2.3. Refractory Mass Inflow Rate

The refractory mass inflow rate, which describes the amount of matter that falls from the matter which is funneled to the star at the X-region, can be expressed via:

$$S = \dot{M}_D \cdot X_r \cdot \varphi \quad (3)$$

Here, \dot{M}_D describes the rate at which mass is accreted onto the disk, X_r describes the cosmic mass fraction, and φ describes the proportion of matter that reaches the X-region, as described in Lee et al. [3]). For \dot{M}_D , we adopt 1×10^{-7} solar masses year^{-1} . For class II and III PMS stars, this value falls at the higher end of estimates, whereas for class 0 and class I PMS stars, it is lower by one to two orders of magnitude. In our model, slower mass accretion rates produce greater SLR concentrations (cf. Bricker & Caffee [13]) for a discussion of disk mass accretion rates for PMS stars). X_r indicates the portion of refractory rock found in the funnel, whereas φ indicates the proportion of mass which drops out of the funnel flow. We set $X_r = 4 \times 10^{-3}$ and $\varphi = 0.01$, which is in accordance with Lee et al. [3]. The value $\varphi = 0.01$ represents the maximum fraction, where this choice assumes that all the refractory matter which forms the planets in the solar system falls from the accretion funnel flow. This is reasonable under the assumption that the funnel flow supplies all the mass that makes up the Sun, and that the rocky component of the planets in the solar system constitutes 0.013 of the Sun's mass [3]. When these values are applied to equation (3), the result is $S = 2.5 \times 10^{14} \text{ g s}^{-1}$.

2.4. SLR Outflow Rate

The physical environment and spatial configuration that determine where the SLRs are produced and what ultimately happens to them is outlined in Bricker and Caffee [13]. Here we give a brief summary. We assert that the SLRs are produced close to the proto-Sun in solar-like flare events, enhanced in luminosity over contemporary levels, and a fraction of the daughter radionuclides are accelerated outward, directed by magnetic field lines, and integrate into the inflowing material, which is too massive and drops out of the main funnel flow. Recent studies support the notion that PMS flaring morphologies are similar to recent solar flare morphologies (cf. Getman et al. [29]). P , described here as the effective rate of SLR out, in units of s^{-1} , can be calculated via:

$$P = p \cdot f \quad (4)$$

Here, p is the cosmogenic rate of production of the daughter nuclei found using equation (1). f describes the proportion of the solar wind radionuclides which becomes incorporated into the where CAIs are formed. After Bricker & Caffee [13], we use $f = 0.1$ for the SWIM calculations, i.e., we assume that 10% of the produced radionuclides are captured into the infalling refractory material. (See Bricker & Caffee [13]) for a discussion of physical setting and geometry, and the parameter f .

3. Results

In eqn. (3) we obtained a refractory rock inflow rate $S = 2.5 \times 10^{14} \text{ g s}^{-1}$. ^{53}Mn content found in the refractory material, calculated via the SWIM, is expressed as:

$$N^{53\text{Mn}} = \frac{P}{S} = \frac{p \cdot f}{\dot{M}_D \cdot X_r \cdot \phi} \quad (5)$$

Here, P is reported in units of atoms s^{-1} and S is reported in units of g s^{-1} .

Tables 3 & 4 show the results of equation (5) using p calculated for ^{53}Mn from equation (1) for various flare compo-

sitions with the parameters described in section 2.1 through 2.2. Figure 1 depicts the predicted $^{53}\text{Mn}/^{55}\text{Mn}$ ratio from the SWIM model per spectral index. Figure 2 depicts predicted $^{53}\text{Mn}/^{55}\text{Mn}$ ratio normalized to “canonical”. Figures 1 and 2 appear on the next page.

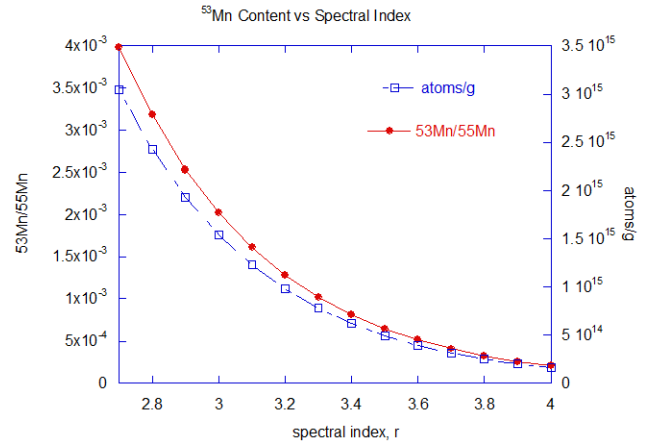


Figure 1. $^{53}\text{Mn}/^{55}\text{Mn}$ ratios & content calculated via the SWIM. The “canonical” ratio of $^{53}\text{Mn}/^{55}\text{Mn}$ is 4×10^{-5} .

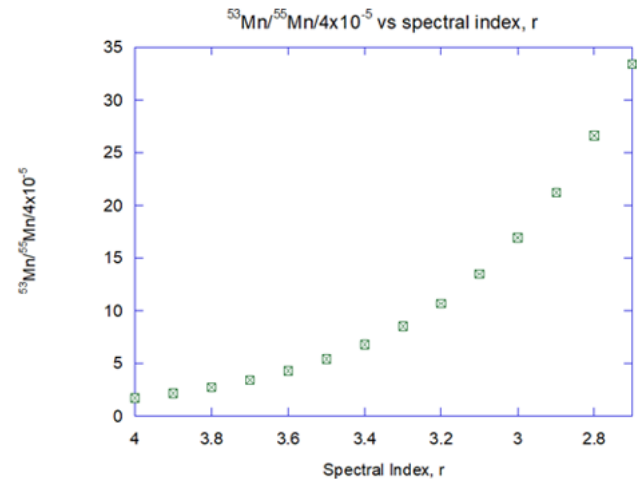


Figure 2. Calculated isotopic ratio of $^{53}\text{Mn}/^{55}\text{Mn}$. A ratio of 1 indicates unity with “canonical”.

Table 3. Predicted Concentration of ^{53}Mn in CAI (atoms g^{-1}).

$r=2.7, {}^3\text{He}/\text{H}=0$	$r=3.3, {}^3\text{He}/\text{H}=0$	$r=4, {}^3\text{He}/\text{H}=0.1$	$r=4, {}^3\text{He}/\text{H}=0.3$
3.0×10^{15}	7.8×10^{14}	1.6×10^{14}	1.6×10^{14}

Table 4. Predicted Isotopic Ratio $^{53}\text{Mn}/^{55}\text{Mn}$.

$r=2.7, {}^3\text{He}/\text{H}=0$	$r=3.3, {}^3\text{He}/\text{H}=0$	$r=4, {}^3\text{He}/\text{H}=0.1$	$r=4, {}^3\text{He}/\text{H}=0.3$
1.3×10^{-3}	3.4×10^{-4}	6.9×10^{-5}	6.9×10^{-5}

4. Discussion

4.1. Uncertainties

As discussed previously, experimental nuclear cross sections were employed whenever possible for calculated ^{53}Mn rates of production in the SWIM. Using cross section data obtained from nuclear model codes yields an uncertainty of at best a factor of two [30]. We assume the target composition for SLR production to be of current solar composition [24]. To represent the concentration of the SLRs calculated originally in atoms g^{-1} as an isotopic ratio for comparison to experimental isotopic ratios, we rely on CAI composition given in table 1. For Be content see McKeegan et al. [10] and Leya et al. [11], and for all other see Leya et al. [11] and sources cited in those publications. The elemental abundances shown are not tightly constrained due to the limited data available on the overall composition of CAIs. We estimate the uncertainty in the composition to be roughly a factor of ~ 2 -3 (cf. Leya et al. [11]). In the SWIM calculations, we used $f = 0.1$, corresponding to 10% of the Mn^{53} produced close to the Sun being integrated at the X-region into CAI precursor material. Because of the inherent uncertainty in the disk spatial geometry, it is not feasible to calculate f from fundamental principles. It is conceivable that a significant amount of 53-manganese would follow magnetic field lines to the X-region, so $f=0.1$ is a conservative estimate. In consideration of S , the rate at which refractory mass inflows, the assumption is a constant disk accretion rate of 1×10^{-7} solar masses year^{-1} , which corresponds to $2.5 \times 10^{14} \text{g s}^{-1}$ of refractory material through the X-region, however disk accretion rates are unconstrained and are likely to change over time (cf. Calvet et al. [31]; Alexander & Armitage [32]). The choice of 1×10^{-7} solar masses year^{-1} is at the upper end of the range for both class II or class III PMS stars, but may be one to three orders of magnitude smaller for these stars (Calvet et al. [31]). On the other hand, the typical rates class I and class 0 PMS stars for may about 10^{-6} or 10^{-5} solar masses year^{-1} for class I and class 0 PMS stars, respectively. Variations in the parameter f and the S inflow rate would systematically affect all the SLR to the same extent. Taking the cross section uncertainties and compositional uncertainties into account, we estimate the overall uncertainty to roughly be a factor of ~ 5 .

The model assumes that radiogenic ^{53}Mn is not altered by aqueous or thermal processes after incorporation. However, measurements of meteorite samples suggest the presence of

alteration processes, which could explain the discrepancies between predicted and measured ratios.

4.2. ^{53}Mn Results

For ^{53}Mn , the model yields a $^{53}\text{Mn}/^{55}\text{Mn}$ isotopic ratio a factor of 2 greater than canonical for $r = 4$, and a factor of 30 greater for $r = 2.7$. Manganese-53 is primarily produced through energetic protons reactions, so a flatter energetic particle energy spectrum naturally leads to more particles above the threshold for the reaction. The spectral index which leads to isotopic ratios consistent with $\sim 10^{-5}$ is $r = 4$.

At the $r = 4$ spectral value, the SWIM over produces 4×10^{-5} by a factor of 2 and over produces the Desch et al. [21] value by a factor of 10. As the ancient $^{53}\text{Mn}/^{55}\text{Mn}$ ratio is not at all well constrained and taking into account the model uncertainty, the SWIM does provide order of magnitude estimate of the original $^{53}\text{Mn}/^{55}\text{Mn}$ isotopic ratio at CAI formation.

The SWIM model assumed that the radiogenic 53-manganese incorporated into the CAIs at the time of formation is not altered through aqueous or thermal processes. Measurements of meteorite samples for the primordial $^{53}\text{Mn}/^{55}\text{Mn}$ ratio in CAIs do indeed show alternative processes [20] and one would expect the ratio found from the SWIM to be larger than measured values. Defining that alteration falls outside the scope of this study.

5. Summary

The solar wind implantation model was used to calculate the predicted initial ratio of $^{53}\text{Mn}/^{55}\text{Mn}$ found in CAIs.

The Swim calculations yielded a $^{53}\text{Mn}/^{55}\text{Mn}$ isotopic ratio that was two times greater than the canonical value of 4×10^{-5} for a spectral index of $r = 4$. For $r = 2.7$, the ratio was 30 times greater than the canonical value. Because ^{53}Mn production primarily occurs through energetic proton reactions, a flatter particle energy spectrum ($r = 2.7$) results in a higher number of particles exceeding the reaction threshold, leading to a higher isotopic ratio. The spectral index that produces an isotopic ratio consistent with $\sim 10^{-5}$ is $r = 4$.

At $r = 4$, the SWIM model overestimates both the canonical $^{53}\text{Mn}/^{55}\text{Mn}$ value and the value reported by Desch et al. [2] by factors of 2 and 10, respectively. However, the ancient $^{53}\text{Mn}/^{55}\text{Mn}$ ratio is not well-defined, and given the uncertainties associated with the model, SWIM still provides a reasonable order of magnitude estimate for the initial isotopic

ratio during CAI formation.

The model assumes that radiogenic ^{53}Mn is not altered by aqueous or thermal processes after incorporation. However, measurements of meteorite samples suggest the presence of alteration processes, which could explain the discrepancies between predicted and measured ratios.

Abbreviations

SLR	Short-Lived Radionuclide
CAI	Calcium-Aluminum Inclusion
SWIM	Solar Wind Implantation Model
SEP	Solar Energetic Particle
GCR	Galactic Cosmic Ray
ONC	Orion Nebular Cluster
PMS	Pre-Main Sequence

Author Contributions

Glynn Bricker is the sole author. The author read and approved the final manuscript.

Conflicts of Interest

The author declares no conflicts of interest.

References

- [1] Gounelle, M., Chaussidon, M., & Montmerle, T. 2007. Irradiation in the early solar system and the origin of short-lived radionuclides. *Comptes Rendus Geoscience* 339: 885-894. <https://doi.org/10.1016/j.crte.2007.09.016>
- [2] Desch, S. J., Srinivasan, G., & Connolly, H. C. 2004. An Interstellar Origin for the Beryllium 10 in Calcium-rich, Aluminum-rich Inclusions. *Astrophysical Journal* 602: 528-542. <https://doi.org/10.1086/380831>
- [3] Lee, T., Shu, F. H., Glassgold, A. E., & Rehm, K. E. 1998. Protostellar Cosmic Rays and Extinct Radioactivities in Meteorites. *Astrophysical Journal* 506: 898-912. <https://doi.org/10.1086/306284>
- [4] Shu, F. H., Shang, H., Gounelle, M., Glassgold, A. & Lee, T. 2001. The Origin of Chondrules and Refractory Inclusions in Chondritic Meteorites. *Astrophysical Journal* 548: 1029-1050. <https://doi.org/10.1086/319018>
- [5] Gounelle, M., Shu, F. H., Shang, H., Glassgold, A. E., Rehm, K. E., & Lee, T. 2006. The Irradiation Origin of Beryllium Radioisotopes and Other Short-lived Radionuclides. *Astrophysical Journal* 640: 1163-1170. <https://doi.org/10.1086/500309>
- [6] Shu, F. H., Nojita, J., Ostriker, E., Wilken, F., Ruden, S., & Lizano, S. 1994. Magnetocentrifugally Driven Flows from Young Stars and Disks. 1: A Generalized Model. *Astrophysical Journal* 429: 781-796. <https://doi.org/10.1086/174363>
- [7] Jaeger, M., Wilmes, S., Kölle, V., Staudt, G., & Mohr, P. 1996. Precision Measurement of the Half-Life of ^7Be . *Physical Review C* 54: 423. <https://doi.org/10.1103/PhysRevC.54.423>
- [8] Chaussidon M., Robert F., & McKeegan K. D. 2006. Li and B isotopic variations in an Allende CAI: Evidence for the in situ decay of short-lived ^{10}Be and for the possible presence of the short-lived nuclide ^7Be in the early solar system. *Geochimica et. Cosmochimica Acta* 70: 224-245. <https://doi.org/10.1016/j.gca.2005.08.016>
- [9] Marhas, K. K., & Goswami, J. N. 2004. Low Energy Particle Production of Short-lived Nuclides in the Early Solar System. *New Astronomy Review* 48: 139-144. <https://doi.org/10.1016/j.newar.2003.11.042>
- [10] McKeegan, K. D., Chaussidon, M., & Robert, F. 2000. Incorporation of Short-Lived ^{10}Be in a Calcium-Aluminum-Rich Inclusion from the Allende Meteorite. *Science* 289: 1334-1337. <https://doi.org/10.1126/science.289.5483.1334>
- [11] Leya, I., Wieler, R., & Halliday, A. N. 2003. The Predictable Collateral Consequences of Nucleosynthesis by Spallation Reactions in the Early Solar System. *Astrophysical Journal* 594: 605-616. <https://doi.org/10.1086/376795>
- [12] Mostefaoui, S., G. W. Lugmair, G. W., & Hoppe, P. 2005. ^{60}Fe : A Heat Source for Planetary Differentiation from a Nearby Supernova Explosion. *Astrophysical Journal* 625: 271-277. <https://doi.org/10.1086/429555>
- [13] Bricker, G. E., & Caffee, M. W. 2010. Solar Wind Implantation Model for ^{10}Be in CAIs. *Astrophysical Journal* 725: 443-449.
- [14] Bricker, G. E. & Caffee, M. W. 2013. Incorporation of ^{36}Cl Into Calcium-Aluminum-Rich Inclusions in the Solar Wind Implantation Model. *Advances in Astronomy* 2013: 1-4. <https://doi.org/10.1155/2013/487606>
- [15] Bricker, G. E. 2019 Early Solar System Solar Wind Implantation of ^7Be into Calcium-Aluminum Rich Inclusions in Primitive Meteorites. *International Journal of Astronomy and Astrophysics*, 9, 12-20. <https://doi.org/10.4236/ijaa.2019.91002>
- [16] Nishiizumi, K. & Caffee, M. W. 2001. Beryllium-10 from the Sun. *Science* 294: 352-354. <https://doi.org/10.1126/science.1062545>
- [17] Feigelson, E. D., Garmire, G. P., & Pravdo, S. H. 2002. Magnetic Flaring in the Pre-Main-Sequence Sun and Implications for the Early Solar System. *Astrophysical Journal* 572: 335-349. <https://doi.org/10.1086/340340>
- [18] Wolk, S. J., Spitzbart, B. D., & Bourke, T. L. 2006. X-Ray and Infrared Point Source Identification and Characteristics in the Embedded, Massive Star-Forming Region RCW 38. *Astronomical Journal* 132: 1100-1125. <https://doi.org/10.1086/505704>
- [19] Lugmair, G., & Shukolyukov, A. 1998. Early Solar System Timescales According to ^{53}Mn - ^{53}Cr Systematics. *Geochimica et. Cosmochimica Acta* 62: 2863-2886. [https://doi.org/10.1016/S0016-7037\(98\)00189-6](https://doi.org/10.1016/S0016-7037(98)00189-6)

- [20] Anand, A., Pape, A., Wille, M., & Mezger, K. 2021. Chronological constraints on the thermal evolution of ordinary chondrite parent bodies from the ^{53}Mn - ^{53}Cr system, *Geochimica et Cosmochimica Acta* 307: 281-301. <https://doi.org/10.1016/j.gca.2021.04.029>
- [21] Desch, S. J., Dunlap, D. R., Williams, C. D., Mane, P., & Dunham, E. T. 2023. Statistical chronometry of Meteorites: II. Initial abundances and homogeneity of short-lived radionuclides. *Icarus*, 402, Article 115611. <https://doi.org/10.1016/j.icarus.2023.115611>
- [22] MacPherson, G. J., Davis, A. M., & Zinner, E. K. 1995. The Distribution of Aluminum-26 in the Early Solar System—A reappraisal. *Meteoritics & Planetary Science* 30: 365-386. <https://doi.org/10.1111/j.1945-5100.1995.tb01141.x>
- [23] Reedy, R. C. & Marti, K. 1991. Solar Cosmic-ray Fluxes During the Last 10 Million Years. In *The Sun In Time*, edited by Sonnet C. P., Giampapa, M. S., and Mathews, M. S. Tucson: University of Arizona Press. pp. 260-278.
- [24] Lodders, K. 2003. Solar System Abundances and Condensation Temperatures of the Elements. *Astrophysical Journal* 591: 1220-1247. <https://doi.org/10.1086/375492>
- [25] Robitaille, P. 2006. The Solar Photosphere: Evidence for Condensed Matter. *Progress in Physics* 2: 17-20.
- [26] Nishiizumi, K., Arnold, J. R., Kohl, C. P., Caffee, M. W., Masarik, J., & Reedy, R. C. 2009. Solar cosmic ray records in lunar rock 64455. *Geochimica et Cosmochimica Acta* 73: 2163-2176. <https://doi.org/10.1016/j.gca.2008.12.021>
- [27] Gensho, R., Nitoh, O., Makino, T., & Honda, M. 1979. Some long-lived and stable nuclides produced by nuclear reactions. *Physics and Chemistry of the Earth* 11: 11-18. <https://doi.org/10.1016/0079-1946%2879%2990003-X>
- [28] Ramaty, R., Kozlovsky, B., & Lingenfelter, R. E. 1996. Light Isotopes, Extinct Radioisotopes, and Gamma-Ray Lines from Low-Energy Cosmic-Ray Interactions. *Astrophysical Journal* 456: 525-540. <https://doi.org/10.1086/176677>
- [29] Getman, K., Feigelson, E., Broos, P., Micela, G., & Garmire, G. 2008a. X-Ray Flares in Orion Young Stars. I. Flare Characteristics. *Astrophysical Journal* 688: 418-455. <https://doi.org/10.1086/592033>
- [30] Michel, R., & Neumann, S. 1998. Interpretation of Cosmogenic Nuclides in Meteorites on the Basis of Accelerator Experiments and Physical Model Calculations. *Earth and Planetary Science* 107: 441-457. <https://doi.org/10.1007/bf02841610>
- [31] Calvet, N., Briceno, B., Hernandez, J., Hoyer, S., Hartmann, L., Sicila-Aguilar, A., Megeath, S. T., & D'Alessio, P. 2005. Disk Evolution in the Orion OB1 Association. *Astronomical Journal* 129: 935-946. <https://doi.org/10.1086/426910>
- [32] Alexander, R. D. & Armitage, P. J. 2006. The Stellar Mass-Accretion Rate Relation in T Tauri Stars and Brown Dwarfs. *Astrophysical Journal* 639: L83-L86. <https://doi.org/10.48550/arXiv.astro-ph/0602059>